THE JOURNAL OF BIOLOGICAL CHEMISTRY VOL. 284, NO. 32, pp. 21626–21636, August 7, 2009
© 2009 by The American Society for Biochemistry and Molecular Biology, Inc. Printed in the U.S.A.

Engulfment of Axon Debris by Microglia Requires p38 MAPK Activity*[S]

Received for publication, April 7, 2009, and in revised form, June 3, 2009 Published, JBC Papers in Press, June 15, 2009, DOI 10.1074/jbc.M109.005603

Tatsuhide Tanaka[1], **Masaki Ueno, and Toshihide Yamashita**[2]

From the Department of Molecular Neuroscience, Graduate School of Medicine, Osaka University, 2-2 Yamadaoka, Suita, Osaka 565-0871, Japan

The clearance of debris after injuries to the nervous system is a critical step for restoration of the injured neural network. Microglia are thought to be involved in elimination of degenerating neurons and axons in the central nervous system (CNS), presumably restoring a favorable environment after CNS injuries. However, the mechanism underlying debris clearance remains elusive. Here, we establish an *in vitro* assay system to estimate phagocytosis of axon debris. We employed a Wallerian degeneration model by cutting axons of the cortical explants. The cortical explants were co-cultured with primary microglia or the MG5 microglial cell line. The cortical neurites were then transected. MG5 cells efficiently phagocytosed the debris, whereas primary microglia showed phagocytic activity only when they were activated by lipopolysaccharide or interferon-β. When MG5 cells or primary microglia were co-cultured with degenerated axons, p38 mitogen-activated protein kinase (MAPK) was activated in these cells. Engulfment of axon debris was blocked by the p38 MAPK inhibitor SB203580, indicating that p38 MAPK is required for phagocytic activity. Receptors that recognize dying cells appeared not to be involved in the process of phagocytosis of the axon debris. In addition, the axons undergoing Wallerian degeneration did not release lactate dehydrogenase, suggesting that degeneration of the severed axons and apoptosis may represent two distinct self-destruction programs. We observed regrowth of the severed neurites after axon debris was removed. This finding suggests that axon debris, in addition to myelin debris, is an inhibitory factor for axon regeneration.

Axon degeneration is an active, tightly controlled, and versatile process of axon segment self-destruction. The lesion-induced degeneration process was first described by Waller (1) and has since been known as Wallerian degeneration (2, 3). This degeneration involves rapid blebbing and fragmentation of an entire axonal stretch into short segments, which are then removed by locally activated phagocytic cells. Phagocytic removal of damaged axons and their myelin sheaths distal to the injury is important for creating a favorable environment for axonal regeneration in the nervous system. Although the debris of degenerated axons and myelin is cleared by phagocytes in the peripheral nervous system (PNS), the debris is removed very slowly in the central nervous system (CNS)[3] (4, 5). This is considered to be one of the obstacles for regeneration of the injured axons in the CNS.

Apoptotic neurons are also engulfed by activated phagocytic cells. Apoptosis is very well documented in the CNS where a significant proportion of neurons undergo programmed cell death (6). To prevent the diffusion of damaging degradation products into surrounding tissues, dying neurons are phagocytosed. In the brain, apoptotic cells are engulfed mainly by the resident population of phagocytes known as microglia. Microglia are generally considered to be immune cells of the CNS (7). They respond to any kind of pathology with a reaction termed "microglial activation." After injuries to the CNS, microglia react within a few hours with a migratory response toward the lesion site.

Although insight into the mechanism of phagocytosis of dying cells by microglia has improved, little is known about the mechanism of clearance of degenerated axons and myelin debris by microglia after axonal injury in the CNS. Interestingly, the axons undergoing Wallerian degeneration do not seem to possess detectable activation of the caspase family (8), suggesting that Wallerian degeneration and apoptosis may represent two distinct self-destruction programs. Thus, the mechanism of microglial phagocytosis of dying cells might be different from that of axon/myelin debris. We aimed to elucidate the mechanism of debris clearance by microglia after an axonal injury. We established an *in vitro* assay system to estimate phagocytosis of degenerated axon debris. We found that p38 mitogen-activated protein kinase (MAPK) was critical for the phagocytic activity of microglia. Treatment with lipopolysaccharide (LPS) or interferon-β (IFN-β) was necessary for the primary microglia to become phagocytic. In addition, clearance of degenerated axon debris allowed axonal growth from the severed neurites, suggesting that removal of the axon debris provides a favorable environment for axonal regeneration.

EXPERIMENTAL PROCEDURES

Cell Cultures—Because the number of primary microglia that can be cultured from neonatal mice is limited, two cell

* This work was supported by a research grant from the National Institute of Biomedical Innovation (05-12) and a Grant-in-Aid for Young Scientists (S) from the Japan Society for the Promotion of Science.

[S] The on-line version of this article (available at http://www.jbc.org) contains supplemental Movie S1.

[1] Present address: Dept. of Functional of Anatomy and Neuroscience, Asahikawa Medical College, Midorigaoka-Higashi 2-1-1-1, Asahikawa 078-8510, Japan. E-mail: ttanaka@asahikawa-med.ac.jp.

[2] To whom correspondence should be addressed. Tel.: 81-6-68793661; Fax: 81-6-68793669; E-mail: yamashita@molneu.med.osaka-u.ac.jp.

[3] The abbreviations used are: CNS, central nervous system; MAPK, mitogen-activated protein kinase; DMEM, Dulbecco's modified Eagle's medium; LDH, lactate dehydrogenase; IFN-β, interferon-β.

culture lines were used. The MG5 microglial cell line derived from p53-deficient mice was cultured in A1-cell conditioned medium (9). A1 cells were cultured in DMEM supplemented with 10% fetal bovine serum. Primary cultures of microglial cells were obtained from Wistar rats on postnatal day 1 (P1). Briefly, the rat cerebral cortex was digested with 0.25% trypsin and 70 units DNase for 15 min. Cells were passed through a 70-μm nylon mesh. The resultant cell suspension was diluted with DMEM supplemented with 10% fetal bovine serum and 1% penicillin/streptomycin and seeded into poly-L-lysine-coated several dishes. Microglial cells from the astrocyte-monolayer sheet were removed by shaking. Briefly, the conditioned medium was collected into the centrifuge tube. The medium-removed dishes were shaken for several times. Then, the medium was gently poured into the dishes and recollected. For cortical explant cultures, the cortex was removed from E14-E16 (C57BL/6J mouse) or E18-E20 (Wistar rat) according to previously reported methods, with a slight modification (10). The cortex was chopped into 300–600-μm-sized pieces using tungsten needles. The chopped cortex pieces were then placed in a 3.5-cm tissue culture dish containing 1 ml of DMEM/F12 supplemented with 10% fetal bovine serum. After 6 days of incubation at 37 °C in a humidified 95% air, 5% CO_2 incubator, the medium was exchanged to DMEM/F12 supplemented with 2% B27 (Invitrogen, Carlsbad, CA). Primary microglia (4×10^5 cells) or MG5 cells (2×10^5 cells) were co-cultured. The extended neurites from the explant cortex culture were transected using a blade.

Reagents for Cell Cultures—The concentrations of reagents used in this study were as follows: 1 μg/ml LPS (Sigma-Aldrich), 300 units/ml IFN-β (Sigma-Aldrich), 50 μM SB203580 (a p38 MAPK inhibitor; Sigma-Aldrich), 100 μM kainic acid (Sigma-Aldrich), 10 μM MRS2578 ($P2Y_6$ receptor antagonist; Sigma-Aldrich), and 0.5 μM staurosporine (BIOMOL, Plymouth Meeting, PA). The cells were pretreated with each inhibitor for 30 min before axotomy.

Time-lapse Imaging—The cortical explants and MG5 cells were co-cultured in a poly-L-lysine-coated dish for 12 h, and the neurites were then transected. The culture dish was then transferred to a heated stage apparatus (model MI-IBC-IF, Olympus, Tokyo, Japan). Time-lapse images were acquired every 8 min for 36 h with an Olympus IX81 microscope using a 10× objective lens. Images were combined into a time-lapsed sequence by using MetaMorph software (Molecular Devices, Sunnyvale, CA).

Fluorescent Immunostaining—Fluorescent immunostaining was performed at the end of the culture time. Cells were fixed in 4% paraformaldehyde in 0.1 M phosphate buffer for 1 h at room temperature and incubated with a blocking solution containing 1% bovine serum albumin and 0.1% Triton X-100 in phosphate-buffered saline for 1 h, followed by overnight incubation at 4 °C with anti-β-tubulin III (Tuj-1) antibody (diluted 1:1000 in the blocking solution; Covance, Princeton, NJ), anti-ED1 (CD68) antibody (diluted 1:100 in the blocking solution; AbD Serotec, Raleigh, NC), anti-GAP43 antibody (diluted 1:1000 in the blocking solution; Chemicon/Millipore, Temecula, CA), and anti-phospho-p38 antibody (diluted 1:100 in the blocking solution; Cell Signaling Technology, Beverly, MA). Fluorescent dye Alexa Fluor 488-conjugated anti-rabbit IgG or 568-conjugated anti-mouse IgG (diluted 1:1000 in phosphate-buffered saline containing 0.1% Triton X-100; Molecular Probes/Invitrogen) was used as the secondary antibody.

Western Blotting—Cells were lysed with 10 mM Tris buffer, pH 7.4, containing 150 mM NaCl, 5 mM EDTA, 1% Triton X-100, 1% deoxycholic acid, 0.1% SDS, 1 mM sodium vanadate, and protease inhibitor mixture (Roche Applied Science). The homogenate was centrifuged at 17,400 × *g* for 10 min, and the supernatant was stored at −20 °C. The protein concentration was measured using a bicinchoninic acid protein assay kit (Pierce). Equal amounts of protein were loaded into each lane, run on sodium dodecyl sulfate (SDS)-polyacrylamide gels, and then transferred to a polyvinylidene difluoride membrane (Millipore). The blots were probed with anti-phospho-MEK1/2 (1:1000; Cell Signaling Technology), anti-MEK1/2 (1:1000; Cell Signaling Technology), anti-phospho-c-Jun N-terminal kinase, (JNK, 1:5000; Promega, Madison, WI), anti-JNK (1:1000; Cell Signaling Technology), anti-phospho-p38 (1:1000; Cell Signaling Technology), and anti-p38 (1:500; Cell Signaling Technology). Immunoblot analysis was performed with horseradish peroxidase-conjugated anti-mouse and anti-rabbit IgG (Cell Signaling Technology) using enhanced chemiluminescence Western blotting detection reagents (GE Healthcare, Piscataway, NJ).

Lactate Dehydrogenase Release—The media of the explant cultures were collected and assayed for lactate dehydrogenase (LDH) activity using a cytotoxicity detection kit (Roche Applied Science). Briefly, LDH catalyzes the conversion of lactate to pyruvate upon reduction of NAD^+ to $NADH/H^+$; the added tetrazolium salt is reduced to formazan. The amount of formazan formed correlates with LDH activity. The formazan product was measured with a microtiter plate reader (Molecular Devices) at 490 nm.

Reverse Transcription-Polymerase Chain Reaction—Total RNA was extracted from the cells or spleen/brain with TRIzol (Invitrogen) and converted to cDNA by reverse transcriptase using a random primer to prime MultiScribe reverse transcriptase (Applied Biosystems) according to the manufacturer's instructions. Specific DNAs were mixed and amplified with 0.2 μM of each primer and cDNA. PCR primers used in this study were as follows: *Tim-4* sense primer, 5′-GGCTCCTTCTCACAAGAAACCACA-3′; *Tim-4* antisense primer, 5′-TCAGCTGTGAAGTGGATGGGAGA-3′; β-actin sense primer, 5′-TGTATGCCTCTGGTCGTACC-3′; and β-actin antisense primer, 5′-CAACGTCACACTTCATGATGG-3′. The PCR cycling conditions for *Tim-4* were 5 min at 96 °C; multiple cycles of 30 s at 96 °C, 30 s at 60 °C, and 30 s at 72 °C; 32 cycles. For β-actin, the PCR-cycling conditions were 5 min at 96 °C; multiple cycles of 30 s at 96 °C, 30 s at 58 °C, and 30 s at 72 °C; 21 cycles. The PCR products were separated by electrophoresis on 1.5% agarose gels and visualized using ethidium bromide.

Statistical Analysis—The significant difference in data in Figs. 1 and 2 was calculated by Student's *t* test. Other data were subjected to one-way analysis of variance, and differences between treatment means were determined by the Tukey-Kramer method.

RESULTS

Establishment of an in Vitro Assay System to Estimate Phagocytosis of Axon Debris—To elucidate the function of microglia in debris clearance following axonal injury, we attempted to establish an assay system for microglial phagocytosis of axon debris *in vitro*. We employed the explant culture of the cerebral cortex from E14-E16 mice. At 6 days after explant culture, when numerous neurites were observed (Fig. 1*A*), we performed transection of the neurites by using a blade (Fig. 1*B*). The severed distal neurites began to develop signs of early degeneration, such as focal swelling and beading, ~8 h after the axons had been separated from their cell bodies, namely, Wallerian degeneration (Fig. 1*C*). When the MG5 murine microglial cell line was co-cultured, the degenerated axon debris was partly cleared by the MG5 cells, whereas proximal neurites remained intact (Fig. 1*D*). To assess whether MG5 cells engulfed degenerating neurites, we immunostained the neurons and MG5 cells by anti-Tuj1 (green) and anti-ED1 (red) antibodies, respectively. The result demonstrated that these signals co-localized 36 h after axotomy (Fig. 1*E*). Thus, degenerated axon debris was cleared by phagocytosis by MG5 cells. Severed neurites became fragmented debris, consisting of microtubules and neurofilaments. We quantified the number of fragmented neurites by counting the Tuj1-positive particles. Quantitative analysis revealed that the residual axon debris was significantly reduced 36 h after transection if MG5 cells were co-cultured (reduced to 25.1% ± 7.4% of control) (Fig. 1*F*). To directly study the dynamic movement of MG5 cells during phagocytosis, we performed time-lapse analysis. The results shown in Fig. 1*G* and supplemental Movie S1 were based on time-lapse observations taken up to 36 h after transection. Live imaging showed that MG5 cells started to clear debris at ~15 h and became highly motile afterward (supplemental Movie 1). Notably, engulfment was specific to the distal part of the severed neurites but not to the proximal part or to the cell bodies (Fig. 2, *A*–*C*). We then traced motile MG5 cells in the proximal (including cell bodies and proximal neurites) and distal (including transected distal neurites) regions from the transected site for up to 32 h and measured the distance of the movement in the two-dimensional field at 0–2, 10–12, 20–22, and 30–32 h (Fig. 2*D*). MG5 cells showed high motility, specifically in the distal region at 10–12 and 20–22 h, although little migration was observed in the proximal region during the observation period. We performed quantitative analysis of the microglial motility. MG5 cells became highly motile in the distal region (47.5 ± 12.6 μm/h) compared with the proximal region (13.3 ± 2.8 μm/h) (Fig. 2*E*). In addition, the cell bodies of some, but not all, MG5 cells in the distal region became hypertrophic in a time-dependent manner (Fig. 2*F*). These observations *in vitro* resembled those *in vivo* after injury to the nervous system. Thus, our *in vitro* assay system is a useful tool to analyze the mechanism of debris clearance by microglial cells.

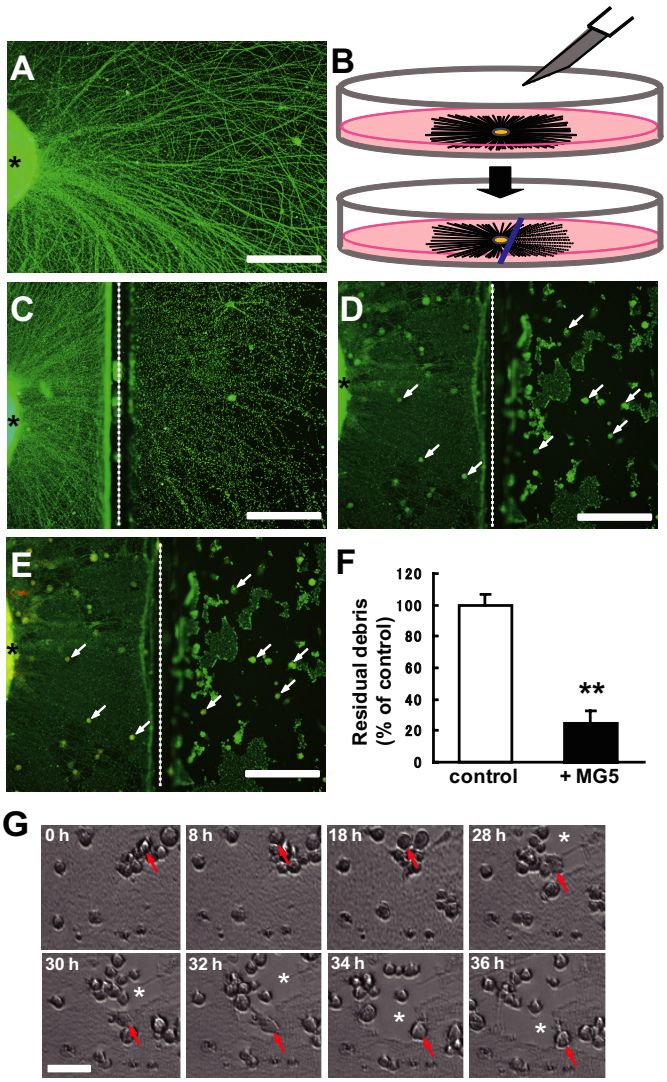

FIGURE 1. **Establishment of an *in vitro* assay system to estimate phagocytosis of axon debris.** *A*, photomicrograph of the explant culture immunostained for neuronal class III β-tubulin, Tuj-1. The neurites extended from the explants in a radial pattern. An *asterisk* indicates the cortical explant. *B*, procedure of transection of the neurites from the explant culture. Briefly, the chopped cortex pieces were placed in a tissue culture dish. After microglial cells were seeded, the axons of cortical explants were cut using a blade (*upper*). Approximately 8 h after axotomy, Wallerian degeneration was observed at the distal neurites from the injury site (*lower*). *C*, photomicrograph of degenerating axons immunostained for Tuj-1. The lesion-induced degeneration process, such as focal swelling and beading 8 h after neurites, was observed. An *asterisk* indicates the cortical explant, and a *dotted line* indicates the transected site (*C*–*E*). *D*, degenerated axons were engulfed by the MG5 microglial cells. Immunofluorescence labeling of Tuj-1 is shown. *E*, double immunostaining for Tuj-1 and ED1 (marker for microglia). *F*, quantitative analysis of the relative number of remaining debris compared with the control (without MG5 cells). The residual axon debris was significantly reduced 36 h after transection when MG5 cells were co-cultured. Data are represented as mean ± S.E. of four independent experiments. **, $p < 0.01$ compared with the control. *G*, time-lapse analysis of phagocytic MG5 cells. *Arrows* indicate a migrating individual cell. When MG5 cells were co-cultured, debris was efficiently cleared by these cells (*asterisks*). *Scale bar* (*A*, *C*, *D*, and *E*) 200 μm; (*G*) 50 μm.

Primary Microglia Require LPS or IFN-β to Become Phagocytic—We examined whether engulfment of degenerating axons was observed in primary cultures of microglia. Because primary microglial cells used in this study were obtained from Wistar rats on postnatal day 1 (P1), we employed the explant culture of the cerebral cortex from E18-E20 rats (6 days of incubation) (Fig. 3, *A* and *B*). Unlike MG5 cells, clearance of the debris was not efficient in primary microglia from rats (Fig. 3, *A* and *B*). Only 26% of the fragmented neurites were engulfed at 144 h after axotomy (compared with 74.9% by MG5

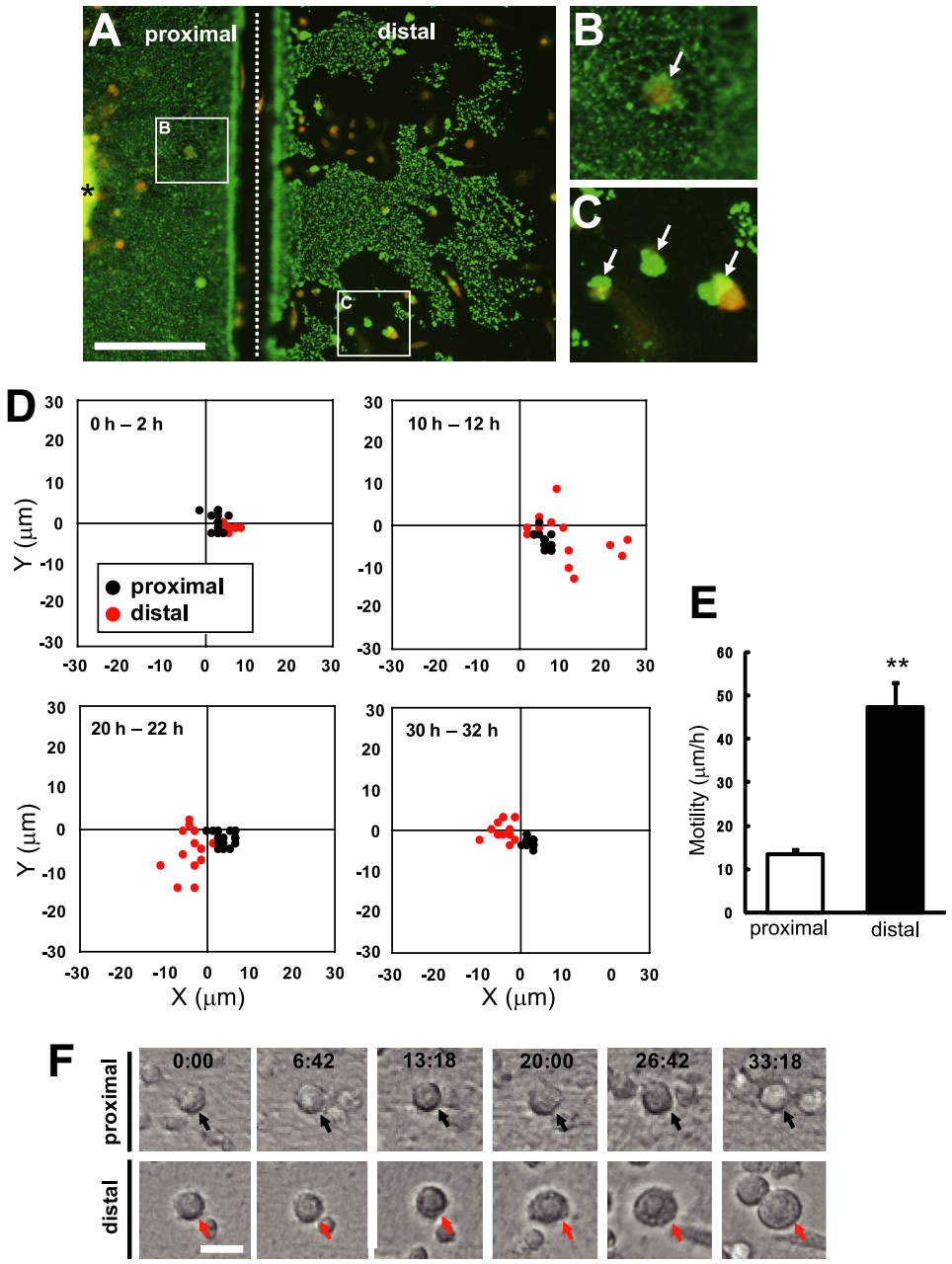

FIGURE 2. **Phagocytic microglia became highly motile and hypertrophic.** *A*, double immunostaining of Tuj-1 and ED1 36 h after transection of axons. Although degenerating axons in the distal part of injury site were phagocytosed by MG5 cells, the proximal axons were not phagocytosed. An *asterisk* indicates the cortical explant, and a *dotted line* indicates injury site. *Scale bar*, 200 μm. *B* and *C*, high magnification views of the boxed regions in *A*. *Arrows* indicate MG5 cells. *D*, measurement of the migration of MG5 cells in the two-dimensional field during the indicated periods. Microglial migration in the distal part of injury site (*red*) was enhanced over 10–12 h and 20–22 h compared with the proximal part (*black*). *E*, quantitative analysis of the motility of MG5 cells in the distal region and proximal region. Motility of MG5 cells over 10–36 h increased in the distal region compared with the proximal region. Data are represented as mean ± S.E. **, $p < 0.01$ compared with the proximal region. *F*, alteration of the morphology of MG5 cells in the proximal and distal part of injury site. Hypertrophy of microglial cell bodies were observed specifically in the distal part of the injury site. *Scale bar*, 30 μm.

cells). This result suggests that neurite debris was not sufficient for induction of phagocytic activity from primary microglia. To assess whether activation of microglia was necessary for engulfment of debris, primary microglia were treated with 1 μg/ml LPS before axotomy. Clearance of the degenerated neurites by the primary microglia was strongly up-regulated by LPS at 96 h (reduced to 50.0% ± 4.2% of unstimulated control microglia) and 144 h (reduced to 8.1% ± 2.4% of unstimulated control microglia). It has been reported that IFN-β enhances the ability of microglia to phagocytose apoptotic T cells, thereby resulting in a suppression of the immune response (11). Therefore, we treated the primary microglia with 300 units/ml IFN-β. Clearance of the degenerated neurites by the primary microglia was also significantly up-regulated, but to a lesser extent than that with the LPS treatment, at 96 h (reduced to 55.7% ± 4.8% of control) and 144 h (reduced to 51.8% ± 2.5% of control). This quantitative analysis showed that a certain amount of time was required for primary microglia to acquire ability for engulfment (Fig. 3*B*). These results suggested that primary microglia are in a resting state *in vitro* and that LPS or IFN-β is required for the acquisition of phagocytic capability. However, it should be noted that activation of primary microglia by LPS or IFN-β is not sufficient for phagocytosis, as these activated microglia did not phagocytose the proximal axons or cell bodies (data not shown). Thus, microglia may need to recognize some signals on the degenerated axons to become phagocytic.

Axon Debris Inhibits Neurite Growth in Vitro—Next, we examined whether clearance of degenerated neurites was necessary for axonal growth from the severed neurites. The cortical explants were cultured for up to 96 h after transection in the presence or absence of MG5 cells, and fluorescent immunostaining was then performed using anti-Tuj1 and anti-ED1 antibodies. We found that numerous extended axons were observed distal to the transected site when degenerated debris was cleared by MG5 cells (Fig. 4, *C* and *D*). In contrast, no fibers could be seen beyond the site of transection if the debris was not cleared in the absence of MG5 cells (Fig. 4, *A* and *B*). Consistent results were obtained in the presence of primary microglia (Fig. 4, *E* and *F*). In this experiment, the cortical explants were cultured for up to 10 days after transection in the presence of primary microglia and LPS, as a certain amount of time was required for primary microglia to acquire the engulfment ability.

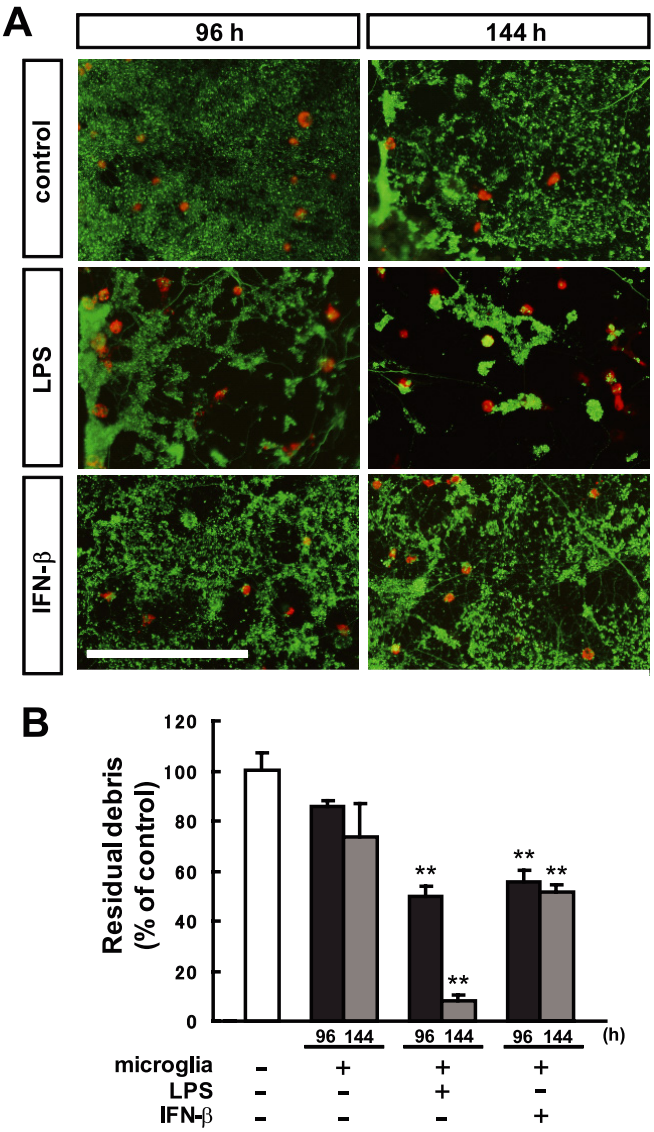

FIGURE 3. **Primary microglia required LPS or IFN-β to become phagocytic.** *A*, double immunostaining for Tuj-1 (*green*) and ED1 (*red*) 96 h and 144 h after transection. Microglial cells were obtained from Wistar rats on postnatal day 1. These microglia were treated with 1 μg/ml LPS or 300 units/ml IFN-β before axotomy and incubated for the indicated times. Each photo shows the distal part of the severed neurites. Clearance of the debris was observed when microglia were treated with LPS or IFN-β. *Scale bar*, 200 μm. *B*, quantitative analysis of the relative number of remaining debris compared with the control (without microglial cells). Data are represented as mean $\pm$ S.E. of three independent experiments. **, $p < 0.01$ compared with the control.

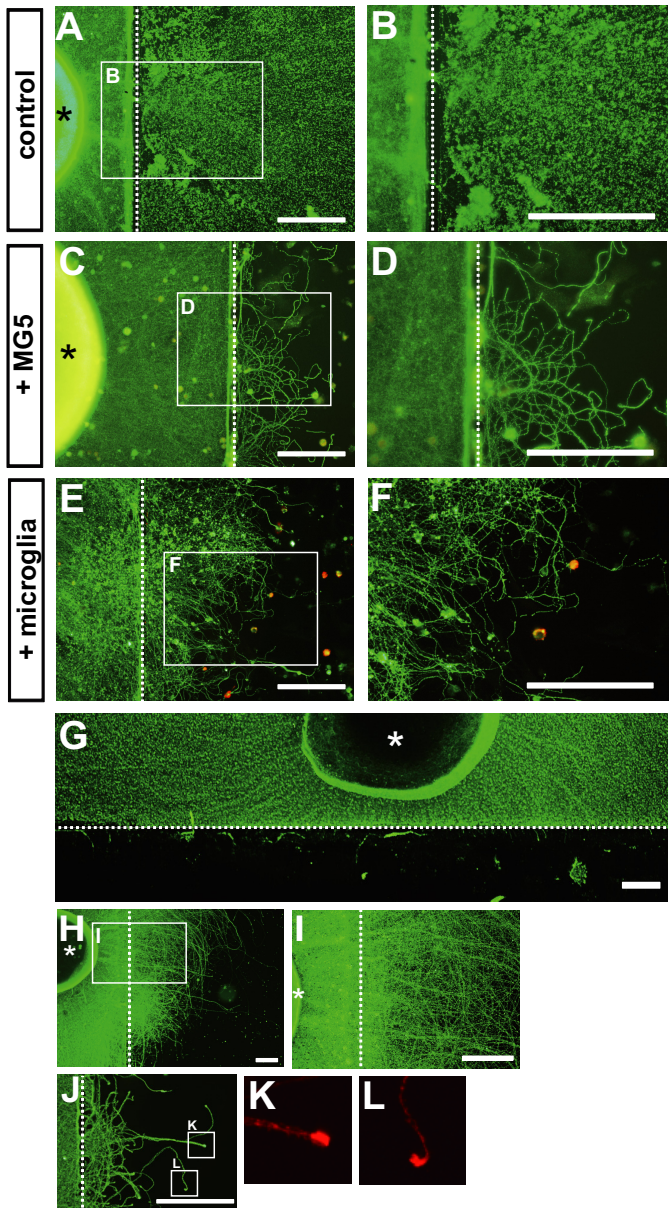

FIGURE 4. **Clearance of the debris allows axon growth *in vitro*.** *A–D*, after transection of the neurites, the cultures were incubated for 96 h in the absence (*A* and *B*) or presence (*C* and *D*) of MG5 cells. Immunostaining was performed using anti-Tuj-1 antibody (*A* and *B*) or anti-Tuj-1 and anti-ED1 antibodies (*C* and *D*). *B* and *D*, higher magnification of the boxed regions in *A* and *C*, respectively. *E*, after transection of the neurites, the cultures were incubated for 10 days in the presence of primary microglial cells stimulated with LPS. *F*, higher magnification of the boxed regions in *E*. *Scale bars*, 200 μm. *G*, degenerating axon debris after transection was removed by a scraper, and immunostaining was then performed using anti-Tuj-1 antibody. *H*, seventy-two hours after the removal of debris, regrowth of the severed axons beyond the site of transection was observed. *I*, higher magnification view of the boxed regions in *H*. *J–L*, growth-associated phosphoprotein (*GAP*)-43 was expressed at the growth cone of the regenerating axons. Immunostaining was performed using anti-Tuj-1 (*green*) and anti-GAP43 antibodies (*red*). An *asterisk* indicates cortical explants, and a *dotted line* indicates the injury site. *Scale bar*, 200 μm.

The above result raised the possibility that axon debris is an inhibitory factor for axon regeneration. Thus, we removed the distal neurites after transection with a scraper (Fig. 4*G*). Growth of the fibers beyond the transected site was observed in a few hours (data not shown). Seventy-two hours after removal of the debris, numerous fibers grew into the distal region from the transected site (Fig. 4, *H* and *I*). Regenerating axons express growth-associated phosphoprotein (GAP)43, which is widely used to specifically label injured neurons and to estimate axonal regeneration (12). We found that GAP43 was expressed at the growth cone of the regenerating axons (Fig. 4, *J–L*). Therefore, regrowth of the severed axons occurred if degenerated distal neurites were cleared. These data suggest that degenerated axon debris is a potent inhibitor of axon regeneration and that removal of the axon debris may provide a favorable environment for axonal regeneration after axonal injuries.

We further examined whether microglia may have a role in enhancing axonal regeneration. After the axon debris was phys-

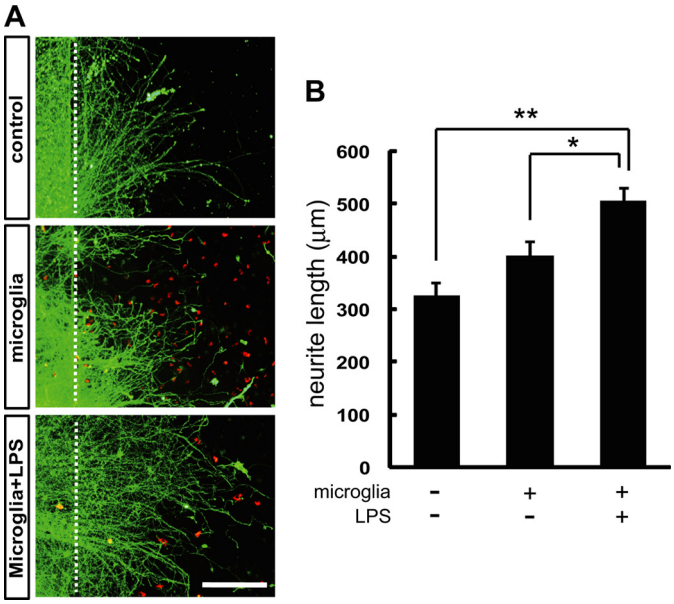

FIGURE 5. **Activated microglia enhance axon growth *in vitro*.** *A*, neurite outgrowth from the transected site in the presence of microglia stimulated with or without LPS. Control; no microglia. *B*, quantitative analysis of the neurite length. Thirty-six hours after removal of the debris, neurite outgrowth from the transected site was increased in the presence of microglia and LPS compared with the control. In the presence of the unstimulated microglia, no significant promotion of neurite growth was observed. Data are represented as mean ± S.E. for at least 50 axons. **, $p < 0.01$; *, $p < 0.05$ compared with the control. *Scale bar*, 200 μm.

ically removed with a scraper, we added microglia in the presence or absence of LPS. Thirty-six hours after removal of the debris, neurite outgrowth from the transected site was increased in the presence of microglia and LPS (504.8 ± 22.8 μm) compared with the control (325.1 ± 24.3 μm) (Fig. 5). In the presence of microglia without LPS, no significant increase in the neurite growth was observed (402.1 ± 25.8 μm) compared with the control (Fig. 5). These results suggest that activated microglia contribute to enhancing axonal regeneration.

p38 MAPK Is Associated with Phagocytic Activity of Microglia—Next, we attempted to explore the signaling pathways that regulate phagocytic activity of microglia. Previous reports have demonstrated that MAPK cascades are involved in microglial activation, which regulates cytokine production (13) and contributes to the generation of neuropathic pain (14). To investigate whether MAPKs are activated in phagocytic microglia, the phosphorylation levels of MEK1/2, JNK, and p38 MAPK were estimated by Western blot analysis using antibodies against the nonphosphorylated and phosphorylated proteins. The cortical explants and MG5 cells were co-cultured for 12 h, and the neurites were then transected. Degenerating axons (without proximal axons) and MG5 cells from 0–48 h after the transection were subjected to Western blot analysis. The phosphorylation level of MEK1/2 was unchanged during the observation period, whereas that of JNK was down-regulated at 12 h and thereafter (Fig. 6, *A* and *B*). However, the phosphorylation level of p38 MAPK in MG5 cells was up-regulated as early as 12 h, and this up-regulation persisted for 24 h (Fig. 6, *A* and *B*). We next examined whether activation of p38 MAPK was required for engulfment of debris. A specific pharmacological p38 MAPK inhibitor, SB203580, was employed to address this question. We found that the p38 MAPK inhibitor significantly blocked engulfment of degenerating neurites by MG5 cells (reduced to 74.0% ± 3.7% of control) (Fig. 6, *C–F*). We further examined whether the phosphorylation of p38 MAPK was observed in microglia or in degenerated axons. We performed immunostaining by using antibodies against the phospho-p38 MAPK and Tuj1 or ED1 14 h after transection. Although immunoreactivity for Tuj1 did not colocalize with that for phospho-p38 MAPK, ED-1-positive MG5 cells were positive for phospho-p38 MAPK (Fig. 6*G*). These results demonstrated that activation of p38 MAPK was observed in MG5 cells, but not in degenerated axons. Consistent with this result, we could not detect the band for phospho-p38 MAPK in the absence of MG5 cells by Western blot (Fig. 6*H*).

We next measured the phosphorylation levels of p38 MAPK by Western blot analysis in primary microglia. The phosphorylation level of p38 MAPK was increased 24 h after transection of axons (Fig. 6, *I* and *J*). As mentioned above, primary microglia are in a resting state *in vitro*, and LPS is required for the activation of primary microglia. Therefore, the above results raised the possibility that phosphorylation of p38 MAPK is induced by LPS. To exclude this possibility, LPS-induced phosphorylation level of p38 MAPK was estimated up to 96 h in primary microglia. As shown in Fig. 6*K*, LPS-induced phosphorylation of p38 MAPK was detected transiently only at 0.5 h after the addition of LPS, but not at 24 h. These results exclude the possibility that LPS directly activated p38 MAPK during phagocytosis of axon debris in primary microglia. In a separate series of experiments, the effect of SB203580 on engulfment of degenerating neurites by LPS-stimulated primary microglia was assessed. LPS-stimulated primary microglia engulfed degenerating axons (reduced to 28.0% ± 4.5% of control), which were partially but significantly blocked by SB203580 (reduced to 53.3% ± 8.1% of control) (Fig. 6, *L–O*). Taken together, these data demonstrated that activation of p38 MAPK was required for engulfment of degenerating axons by primary microglia and MG5 cells.

The Mechanism of Microglial Recognition of Axon Debris Appears to Be Different from That of Apoptotic Cells—Because clearance of the proximal neurites from the transected site was not observed, our results demonstrated that activated primary microglia as well as MG5 cells recognized specifically degenerated debris. Thus, we assumed that the binding of some ligand(s) on the debris to some receptor(s) on the microglia initiated the phagocytic process. We hypothesized that receptors recognizing apoptotic cellular material such as phosphatidylserine (15, 16) might be involved in this process. These receptors include T-cell immunoglobulin-and mucin-domain-containing molecule-4 (Tim-4) and brain-specific angiogenesis inhibitor 1 (BAI1). It has been reported that the expression level of Tim-4 in the brain is very weak compared with that in the spleen, thymus, lymph nodes, and salivary glands (15). In the present study, we obtained results that were consistent with these findings (Fig. 7*A*, *left*). Next, we examined the *Tim-4* mRNA expression in MG5 cells before and after axotomy. As shown in Fig. 7*A*, the expression level of *Tim-4* mRNA in MG5 cells was very low in the control state and was not changed after transection of the neurites (Fig. 7*A*, *right*). The next hypothesis we tested was that the microglial receptor could function as a

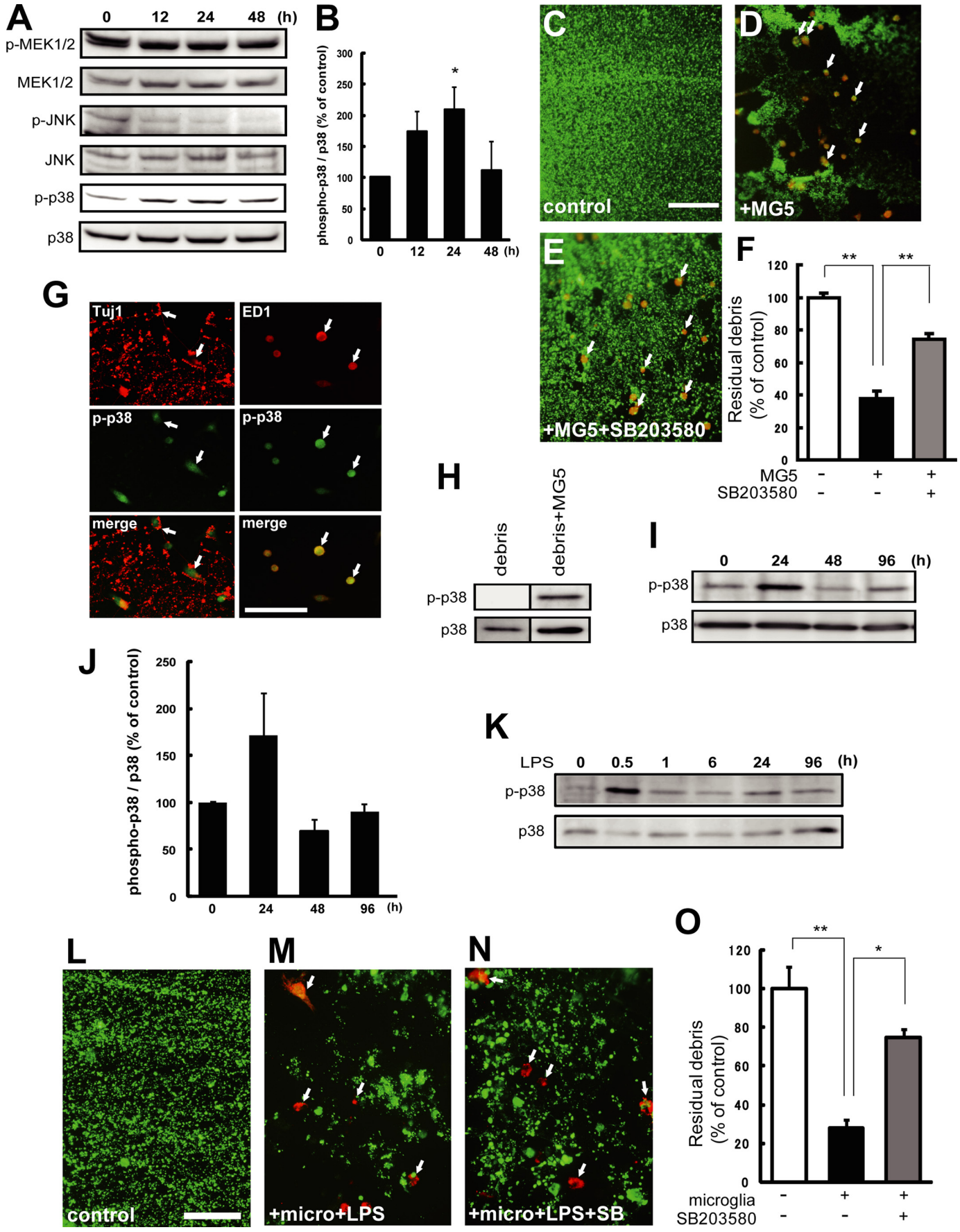
A
0
12
24
48 (h)
p-MEK1/2
MEK1/2
p-JNK
JNK
p-p38
p38
B
phospho-p38 / p38 (% of control)
300
250
200
150
100
50
0
*
0
12
24
48 (h)
C
control
D
+MG5
E
+MG5+SB203580
F
Residual debris (% of control)
120
100
80
60
40
20
0
**
**
MG5 - + +
SB203580 - - +
G
Tuj1
ED1
p-p38
p-p38
merge
merge
H
debris
debris+MG5
p-p38
p38
I
0
24
48
96 (h)
p-p38
p38
J
phospho-p38 / p38 (% of control)
250
200
150
100
50
0
0
24
48
96 (h)
K
LPS 0 0.5 1 6 24 96 (h)
p-p38
p38
L
control
M
+micro+LPS
N
+micro+LPS+SB
O
Residual debris (% of control)
120
100
80
60
40
20
0
**
*
microglia - + +
SB203580 - - +

sensor for phagocytosis by sensing diffusible factors. It has been reported that the microglial metabotropic $P2Y_6$ receptor recognizes the nucleotide UDP released from kainic acid (KA)-treated dying neurons and stimulates microglial phagocytosis (17). We examined whether the microglial $P2Y_6$ receptor contributed to engulfment of degenerating axons. As shown in Fig. 7, *B–E*, MG5 cells engulfed degenerating axons (reduced to 37.6% ± 4.8% of control) that were not blocked by the $P2Y_6$ receptor antagonist MRS2578 (10 μM) (reduced to 43.8% ± 3.7% of control). However, MG5 cells engulfed staurosporine-induced apoptotic neurons, which were partially blocked by MRS2578 (Fig. 7, *F–H* and *J*). These results exclude the possibility that the $P2Y_6$ receptor is necessary for microglial cells to be phagocytic of degenerated axons after transection. We also found that the p38 MAPK inhibitor significantly blocked engulfment of dead neurons by MG5 cells (Fig. 7, *I* and *J*). Interestingly, the axons undergoing Wallerian degeneration did not seem to possess detectable activation of the caspase family (8). We also confirmed that KA induced LDH release in apoptotic cells but that degenerating axons did not release LDH (Fig. 7*K*). These results suggest that there are different mechanisms of microglial phagocytosis between dying neurons and degenerating axons and that Wallerian degeneration and apoptosis may represent two distinct self-destruction programs.

DISCUSSION

In the present study, we established a new assay system to estimate phagocytosis of axon debris by microglia *in vitro*. Some of the key events during *in vivo* microglial activation appeared to occur in our system. Microglia efficiently engulfing the axon debris in this system showed high motility and morphological changes similar to the reported observations *in vivo* (18, 19). Interestingly, clearance of degenerated axons allowed axonal regrowth. This result suggests that degenerated axon debris is a potent inhibitory factor of axon regeneration and that phagocytic removal of axon debris by microglia is important for creating a regenerative environment within the CNS. Why can the axons regenerate from injury site simply by clearance of degenerating debris? Axon debris may express some inhibitory factors for regeneration of the injured axons. Indeed, we have preliminary data to support this hypothesis (data not shown). Another possibility is that degenerating debris become a physical barrier for regeneration of the injured axons.

Our assay enabled us to screen molecules involved in microglial phagocytosis. We found that activation of p38 MAPK is necessary for phagocytosis of degenerating axons. p38 MAPK is activated in spinal microglia after nerve injury and contributes to the development and maintenance of neuropathic pain (14, 20). Phagocytosis of amyloid-β (Aβ) by microglia is dependent on the activation of NF-κB and/or p38 MAPK via the Toll-like receptor (TLR)-4 (21). Recent data have shown that phosphatidylinositol 3-kinase and p38 MAPK are involved in LPS-induced microglial phagocytosis of fluorescent material-conjugated *Escherichia coli* (*E. coli*) particles (22). LPS binds to TLR-4, which is a type I transmembrane protein whose cytoplasmic signaling domain is known as Toll-interleukin-1 receptor (TIR) (23) and activates NF-κB as well as p38 MAPK and JNK. In our assay system, p38 MAPK was activated during engulfment of degenerating axons by microglia after transection of the axons of the cortical explants without use of LPS in MG5 cells. p38 MAPK might be activated independent of the LPS-TLR signaling pathway during phagocytosis of axon debris, as the expression of *TLR4* mRNA in MG5 cells was not induced after transection of the neurites (data not shown). We assume that microglia recognize some molecules on axon debris and become phagocytic through p38 MAPK activation. The phosphorylation level of p38 MAPK was elevated 24 h after transection of axons in primary microglia, and returned to the control level at 48 and 96 h. Thus, activation of p38 MAPK may be required for microglia to become phagocytic, but not for maintaining phagocytic activity. Interestingly, SB203580 did not completely block engulfment of degenerating neurites by primary microglia as well as MG5 cells, as shown in Fig. 6, *F* and *O*, suggesting that other signaling molecule(s) may additively be involved in the process.

Primary microglia showed less phagocytic activity toward axon debris than MG5 cells. However, stimulation of the primary microglia with LPS or IFN-β greatly improved the phagocytic activity. These results demonstrate that primary micro-

FIGURE 6. **Activation of p38 MAPK is necessary for the phagocytic activity of microglia.** *A*, Western blot analysis for various MAPKs. Co-cultures of cortical explants and MG5 cells were incubated for 12 h, and neurites were then transected. Degenerating axons and MG5 cells were collected for the indicated times. Cell lysates were analyzed by immunoblot using antibodies against phosphorylated and nonphosphorylated MEK1/2, c-Jun N-terminal kinase (JNK), or p38 MAPK. The phosphorylation level of p38 MAPK in MG5 cells was up-regulated at 12 h and later. *B*, quantitative analysis of the p38 MAPK phosphorylation level. Levels of phosphorylated p38 MAPK/non-phosphorylated p38 MAPK were determined. Data are represented as mean ± S.E. of three independent experiments. *, $p < 0.05$ compared with the control. *C–E*, effects of SB203580 on phagocytosis of degenerating axons by MG5 cells. SB203580 (50 μM) was added to the culture medium 30 min before transection of the neurites. Double immunostaining of Tuj-1 and ED1 was performed at 36 h after transection of the neurites. MG5 cells engulfed degenerating axons, which were blocked by SB203580. Each panel was obtained from the distal part of the severed neurites. *Arrows* indicate MG5 cells. *Scale bar*, 200 μm. *F*, quantitative analysis of the relative number of remaining debris compared with the control (without MG5 cells). Data are represented as mean ± S.E. of three independent experiments. *, $p < 0.05$ compared with the control. *G*, double immunostaining for p38 MAPK and Tuj-1 or ED1. Immunoreactivity for phospho-p38 MAPK was observed in ED1-positive MG5 cells, whereas no colocalization of the signals for Tuj-1 and phospho-p38 MAPK was found. *H*, Western blot analysis of p38 MAPK and phospho-p38 MAPK in the presence or absence of MG5 cells. *I*, Western blot analysis for p38 MAPK and phospho-p38 MAPK. Co-cultures of cortical explants and primary microglia were incubated for 12 h in the presence of LPS (1 μg/ml), and neurites were then transected. Degenerating axons and primary microglia were collected for the indicated times. The phosphorylation level of p38 MAPK in primary microglia was up-regulated at 24 h. *J*, quantitative analysis of the p38 MAPK phosphorylation level. Data are represented as mean ± S.E. of three independent experiments. *K*, LPS-induced phosphorylation of p38 MAPK in primary microglia. Phosphorylation level of p38 MAPK was detected at 0.5 h after the addition of LPS. Representative data is shown ($n = 3$). *L–N*, effects of SB203580 on phagocytosis of degenerating axons by primary microglia. Primary microglia were treated with 1 μg/ml LPS before addition of SB203580. SB203580 (50 μM, SB) was added to the culture medium 30 min before transection of the neurites and added every 24 h for 4 days. Double immunostaining of Tuj-1 and ED1 was performed at 96 h after transection of the neurites. Each panel was obtained from the distal part of the severed neurites. *Arrows* indicate primary microglia. *Scale bar*, 50 μm. *O*, quantitative analysis of the relative number of remaining debris compared with the control (without primary microglia). Data are represented as the mean ± S.E. of three independent experiments. **, $p < 0.01$; *, $p < 0.05$ compared with the control.

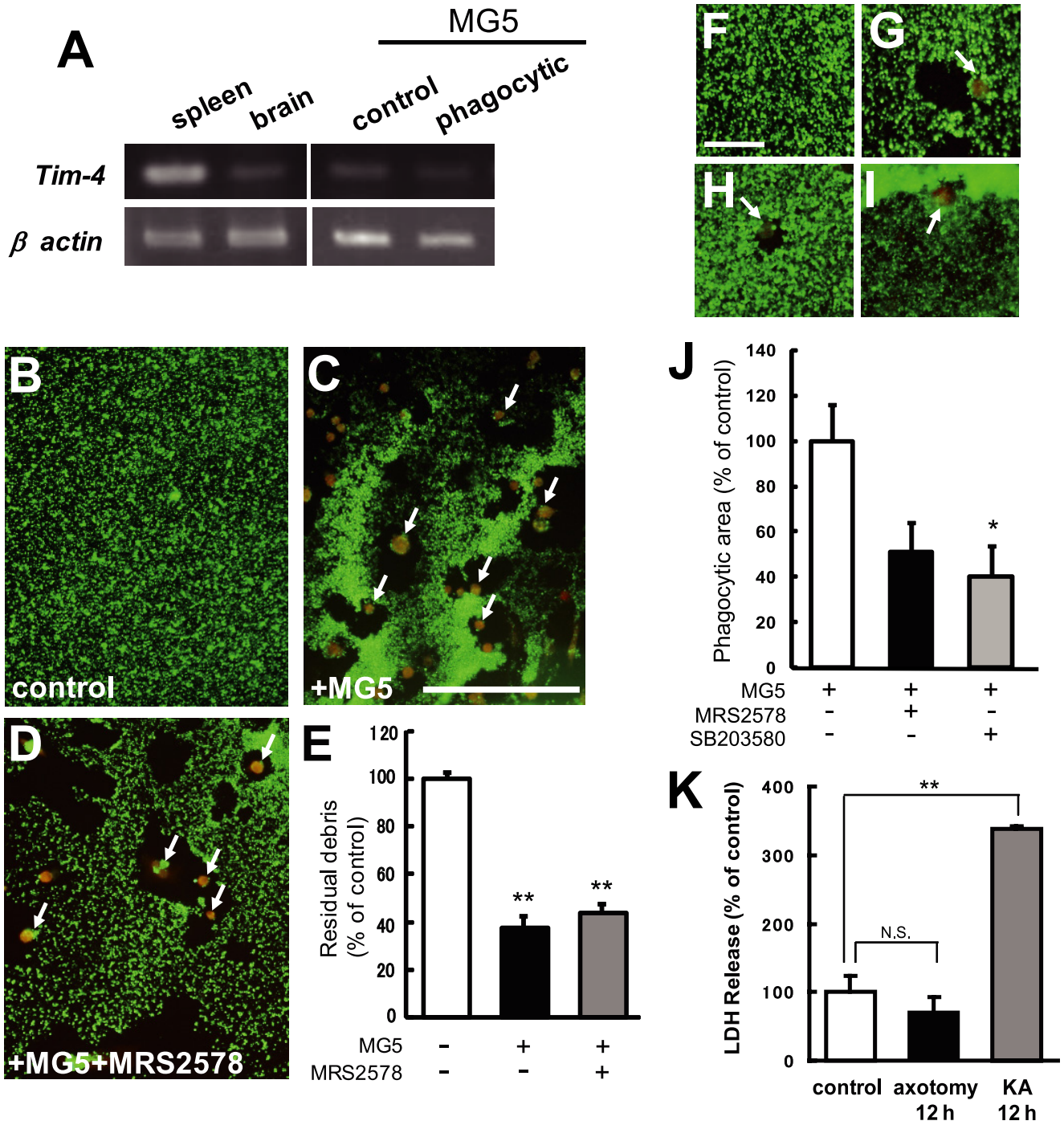

FIGURE 7. **The mechanism of microglial recognition of axon debris appeared to be different from that of apoptotic cells.** *A*, expression profile of *Tim-4* mRNA in C57BL/6J mouse spleen, brain, and MG5 cells. The spleen and brain were obtained from a 7-week-old mouse (*left panels*). The MG5 cells were co-cultured for 0 h (*control*) or 36 h after transection of the neurites (phagocytic) (*right panels*). Representative data for RT-PCR for *Tim-4* transcripts are shown. *B–D*, effects of MRS2578, $P2Y_6$ receptor antagonist, on the phagocytosis of degenerating axons by MG5 cells. MRS2578 (10 μM) was added to the culture medium 30 min before transection of the neurites. Double immunostaining of Tuj-1 and ED1 was performed at 36 h after transection of the neurites. MG5 cells engulfed degenerating axons, which were not blocked by MRS2578. Each panel was obtained from the distal part of the severed neurites. *Arrows* indicate MG5 cells. *Scale bar*, 200 μm. *E*, quantitative analysis of the relative number of remaining debris compared with the control (without MG5 cells). Data are represented as mean ± S.E. of three independent experiments. **, $p < 0.01$ compared with the control. There is no significant difference between MG5 cells and MG5 cells plus MRS2578. *F–I*, involvement of $P2Y_6$ receptor and p38 MAPK in microglial engulfment of staurosporine-induced apoptotic neurons. The neurons were treated with staurosporine for 48 h. *F*, control. *G*, MG5 cells. *H*, MG5 cells treated with MRS2578. *I*, MG5 cells treated with SB203580. *Scale bar*, 50 μm. *J*, quantitative analysis of the phagocytic area of the data in *G–I*. *K*, quantitative analysis of the LDH release in apoptotic cells and degenerating axons. Data are represented as mean ± S.E. of three independent experiments. **, $p < 0.01$ compared with the control. *NS*, not significantly different.

glia are in the resting state, and that some cytokines or soluble factors are required for acquisition of phagocytic activity. Consistent with this observation *in vitro*, systemic injection of LPS accelerates phagocytic activity during Wallerian degeneration in the injured CNS (24). However, it should be noted that these activated microglia still recognized only axon debris but not

proximal axons, strongly suggesting that LPS or IFN-β is not sufficient to induce phagocytosis, and that there should be a mechanism of debris recognition. Further, microglia secrete a variety of cytokines and soluble factors, including endotoxins and chemokines, in response to physiological stimuli (19, 7). Previous studies have shown that p38 MAPK activation results in increased expression of secreted inflammatory mediators/growth factors, such as IL-1β, IL-6, TNF-α, or BDNF, through the transcription factor NF-κB or ATF-2 (20). It is well known that glial cells secrete a number of growth factors and cytokines, including BDNF and leukemia inhibitory factor (LIF), following PNS injury (25). Thus, these secreted factors may affect the growth of the severed neurites as well as their own phagocytic activity. If this is the case, phagocytic microglia may provide a favorable environment for restoration of the injured neural network by multiple functions. Consistent with this notion, we observed that axon regeneration was facilitated by activated microglia.

Clearance of apoptotic cells is crucial to avoid the diffusion of damaging degradation products into surrounding tissues (26). Phosphatidylserine on the surface of apoptotic cells is considered to be a ligand expressed on phagocytes. Recently, two groups reported identification of phosphatidylserine receptors, Tim-4 and BAI1 (15, 16). BAI1, which is regulated by p53, recruits a Rac-GEF complex to mediate the uptake of apoptotic cells. However, because MG5 cells used in this study were established from p53(−/−) homozygote mice (9), BAI1-independent phagocytic pathways should have been responsible for engulfment of degenerating axons, at least by MG5 cells. Furthermore, the expression level of *Tim-4* remained very low during engulfment of degenerating axons, as shown in Fig. 7*A*. Thus, Tim-4 that recognizes dying neurons appeared not to be involved in the process of phagocytosis of the axon debris, although we could not exclude the possibility that low level of Tim-4 was sufficient for activating the phagocytic signals. The axons undergo degeneration without the death of the parent neurons in response to local neurotrophin deprivation. In addition, the axons undergoing Wallerian degeneration do not exhibit hallmarks of apoptosis (8). These results suggest that Wallerian degeneration and apoptosis may represent two distinct self-destruction programs. Therefore, we assume that the ligands and receptors for phagocytosis of the dying cells may be different from those for phagocytosis of the axon debris. However, the p38 MAPK inhibitor significantly blocked engulfment of dead neurons by MG5 cells. Thus, there may be a common intracellular pathway leading to engulfment of axon debris and dying neurons. Identification of the molecules that activate the signals for phagocytosis of the axon debris will be the next step.

Myelin in the CNS contains several growth inhibitory molecules such as MAG, Nogo, OMgp, and RGMa, which exhibit inhibitory effects on axonal regrowth (27–30). Thus, rapid removal of myelin-associated inhibitors is essential for establishing an environment beneficial for axonal regeneration after CNS injury. However, degenerating debris of myelin is removed only very slowly in the CNS compared with PNS (4, 5). It should be noted that the assay system we employed in the present study lacks myelin which plays the central role in the generation of a non-permissive environment. Thus, our data suggest that axon debris is another inhibitory factor for axon regeneration because the debris inhibited the growth of the severed neurites *in vitro*. Therefore, elucidation of the mechanism of phagocytosis of the debris may be useful in developing therapeutic agents against CNS injuries.

In summary, we established an efficient *in vitro* assay system to estimate microglial phagocytosis and identified p38 MAPK as a requirement for the phagocytic activity. We observed regrowth of the severed neurites after elimination of the axon debris, suggesting that axon debris is another inhibitory factor for axon regeneration. This assay system will be useful in finding the ligands on the debris, receptors on microglia, and the downstream molecular events that involve p38 MAPK.

Acknowledgment—We thank Kazutoshi Kiuchi (Gifu University) for the gift of the MG5 microglial cell line.

REFERENCES

1. Waller, A. (1850) *Phil. Trans. R Soc. Lond.* **140,** 423–429
2. Raff, M. C., Whitmore, A. V., and Finn, J. T. (2002) *Science* **296,** 868–871
3. Coleman, M. (2005) *Nat. Rev. Neurosci.* **6,** 889–898
4. George, R., and Griffin, J. W. (1994) *Exp. Neurol.* **129,** 225–236
5. Stoll, G., and Jander, S. (1999) *Prog. Neurobiol.* **58,** 233–247
6. Kuan, C. Y., Roth, K. A., Flavell, R. A., and Rakic, P. (2000) *Trends Neurosci.* **23,** 291–297
7. Hanisch, U. K., and Kettenmann, H. (2007) *Nat. Neurosci.* **10,** 1387–1394
8. Finn, J. T., Weil, M., Archer, F., Siman, R., Srinivasan, A., and Raff, M. C. (2000) *J. Neurosci.* **20,** 1333–1341
9. Ohsawa, K., Imai, Y., Nakajima, K., and Kohsaka, S. (1997) *Glia* **21,** 285–298
10. Yamagishi, S., Fujitani, M., Hata, K., Kitajo, K., Mimura, F., Abe, H., and Yamashita, T. (2005) *J. Biol. Chem.* **280,** 20384–20388
11. Chan, A., Seguin, R., Magnus, T., Papadimitriou, C., Toyka, K. V., Antel, J. P., and Gold, R. (2003) *Glia* **43,** 231–242
12. Goslin, K., Schreyer, D. J., Skene, J. H., and Banker, G. (1988) *Nature* **336,** 672–674
13. Bhat, N. R., Zhang, P., Lee, J. C., and Hogan, E. L. (1998) *J. Neurosci.* **18,** 1633–1641
14. Tsuda, M., Mizokoshi, A., Shigemoto-Mogami, Y., Koizumi, S., and Inoue, K. (2004) *Glia* **45,** 89–95
15. Miyanishi, M., Tada, K., Koike, M., Uchiyama, Y., Kitamura, T., and Nagata, S. (2007) *Nature* **450,** 435–439
16. Park, D., Tosello-Trampont, A. C., Elliott, M. R., Lu, M., Haney, L. B., Ma, Z., Klibanov, A. L., Mandell, J. W., and Ravichandran, K. S. (2007) *Nature* **450,** 430–434
17. Koizumi, S., Shigemoto-Mogami, Y., Nasu-Tada, K., Shinozaki, Y., Ohsawa, K., Tsuda, M., Joshi, B. V., Jacobson, K. A., Kohsaka, S., and Inoue, K. (2007) *Nature* **446,** 1091–1095
18. Kreutzberg, G. W. (1996) *Trends Neurosci.* **19,** 312–318
19. Garden, G. A., and Möller, T. (2006) *J Neuroimmune Pharmacol.* **1,** 127–137
20. Ji, R. R., and Suter, M. R. (2007) *Mol. Pain* **3,** 33
21. Kakimura, J., Kitamura, Y., Takata, K., Umeki, M., Suzuki, S., Shibagaki, K., Taniguchi, T., Nomura, Y., Gebicke-Haerter, P. J., Smith, M. A., Perry, G., and Shimohama, S. (2002) *FASEB J.* **16,** 601–603
22. Sun, H. N., Kim, S. U., Lee, M. S., Kim, S. K., Kim, J. M., Yim, M., Yu, D. Y., and Lee, D. S. (2008) *Biol. Pharm. Bull.* **31,** 1711–1715
23. O'Neill, L. A., and Dinarello, C. A. (2000) *Immunol. Today* **21,** 206–209
24. Vallières, N., Berard, J. L., David, S., and Lacroix, S. (2006) *Glia* **53,** 103–113

25. Boyd, J. G., and Gordon, T. (2003) *Mol. Neurobiol.* **27,** 277–324
26. Lauber, K., Blumenthal, S. G., Waibel, M., and Wesselborg, S. (2004) *Mol. Cell* **14,** 277–287
27. Mukhopadhyay, G., Doherty, P., Walsh, F. S., Crocker, P. R., and Filbin, M. T. (1994) *Neuron* **13,** 757–767
28. Chen, M. S., Huber, A. B., van der Haar, M. E., Frank, M., Schnell, L., Spillmann, A. A., Christ, F., and Schwab, M. E. (2000) *Nature* **403,** 434–439
29. Wang, K. C., Koprivica, V., Kim, J. A., Sivasankaran, R., Guo, Y., Neve, R. L., and He, Z. (2002) *Nature* **417,** 941–944
30. Hata, K., Fujitani, M., Yasuda, Y., Doya, H., Saito, T., Yamagishi, S., Mueller, B. K., and Yamashita, T. (2006) *J. Cell Biol.* **173,** 47–58